EXERGY ANALYSIS AND MACHINE LEARNING FOR ENHANCED EAF STEEL RECYCLING

Jelena B. IVANOVIĆ[1], Vaso D. MANOJLOVIĆ*[1], Nataša M. GAJIĆ[2], Nigel T. PHUTHI[3], Jelena P. ZAKONOVIĆ[4], Miroslav D. SOKIĆ[5], Željko J. KAMBEROVIĆ[1]

[1]University of Belgrade, Faculty of Technology and Metallurgy, Belgrade, Serbia

[2]Innovation centre of the Faculty of Technology and Metallurgy Ltd., Belgrade, Serbia

[3] University of Pretoria, Faculty of Materials and Metallurgical Engineering, South Africa

[4]Metalfer Ltd., Belgrade, Serbia

[5]Institute for Technology of Nuclear and other Mineral Raw Materials, Belgrade, Serbia

[*] Corresponding author; v.manojlovic@tmf.bg.ac.rs

This study relies on exergy principles to analyze the sustainability of the steel recycling process in electric arc furnaces. Focusing on a balance between material and energy efficiencies, the research addresses the degradation of elements such as manganese and silicon from steel to slag phase. Machine learning techniques were employed to predict and optimize element distribution coefficients. By leveraging HSC v. 9 software, a detailed exergy analysis was performed, utilizing precise coefficients for element distribution in steel and slag, with energy consumption. The results demonstrate the potential of integrating exergy analysis and machine learning to enhance the sustainability of steel production, aligning with circular economy principles.
Key words: electric arc furnace, exergy analysis, carbon footprint, circular economy.

1. Introduction

The global steel industry is currently facing significant environmental challenges. This industry contributes significantly to carbon dioxide emissions, accounting for 7-9% of total global emissions. This is further linked to significant energy consumption, representing 20% of total industrial energy consumption [1]. Traditional linear economic models prevalent in steel production exacerbate these problems, characterized by a "take-make-dispose" approach that leads to excessive resource use and significant environmental degradation. Although these models have historically been efficient in meeting market demand, they now face numerous sustainability issues, particularly considering increasing global environmental awareness and regulatory pressures [2].

In response to these challenges, the circular economy (CE) emerges as a transformative model, moving away from traditional linear practices. It is based on the principles of resource efficiency, recycling, and sustainability while extracting maximum value from materials. This model holds significant potential for the secondary steel industry, which annually produces an average of 160 million tons

of steel at over five hundred locations in the European Union. This industry faces increasing costs and quality issues due to material diversity and the deteriorating quality of steel scrap [3].

To effectively implement the circular economy, it is essential to have a sophisticated and agile metallurgical infrastructure. Understanding the distribution of metals and materials throughout the system is crucial, as is the availability of relevant physical, metallurgical, and thermodynamic data. The digitalization of these data allows for the representative modeling and simulation of the movement of metals, materials, and mixtures, accounting for losses that are often ignored. Recognizing these losses is vital to avoid overoptimistic estimations of resource efficiency and the economic viability of the CE system [4-5].

Exergy analysis is a powerful tool for evaluating the efficiency and sustainability of industrial processes, particularly in the context of the circular economy. It quantifies the quality of energy and material flows, enabling the identification of losses and the potential for improvement. Integrating exergy analysis with circular economy principles can significantly enhance the sustainability of steel production by promoting closed-loop recycling, minimizing waste, and improving resource efficiency [6-8].

The circular economy is usually presented as an ideal approach, yet there are considerable challenges. High-profile publications frequently emphasize closed loops while largely ignoring losses and residue formation that occur at all stages of the CE life cycle. These losses destroy exergy and are not limited to the end-of-life stage, underscoring the importance of a realistic and comprehensive approach to implementing circular economy principles [3].

This study aims for a balance between material and energy efficiencies in Electric Arc Furnaces (EAF), with a specific focus on controlling the degradation of elements such as manganese (Mn) and silicon (Si) in molten steel. HSC 9.9.2.3 software [9] was used to obtain thermodynamic data and, alongside real operational data and machine learning techniques, the coefficients for element distribution in steel and slag were obtained. By leveraging exergy analysis, we seek to provide a comprehensive assessment of the sustainability of the EAF process, aligning with the broader goals of the circular economy to reduce the carbon footprint and enhance the efficiency of steel recycling.

2. Methods

2.1. Heating conditions in an electronic furnace

For the calculations, real data from a melting process in a furnace with a capacity of 60 tons of liquid steel and a 60 MVA transformer were used. The diameter of the metal bath (D) is 4100 mm, and the depth (H) is 920 mm. The D/H ratio of 4.45 is lower than the typical range of 4.8 to 6.2. This lower ratio is associated with increased radiation heat losses, energy losses through water cooling, and a reduced intensity of reactions between slag and steel. On the other hand, by insulating and improving heat distribution, foamy slag can mitigate the effects of lower D/H ratios.

The electrodes are of ultra-high power type and are controlled automatically with a separate control system.

The total energy input is from electrical and chemical sources, with about half going towards melting scrap material and 25-30% going to gases and dust. Figure 1 shows the setup of material flows in HSC Chemistry v. 9 software package. The chemical energy is primarily derived from natural gas, the reaction of oxygen with carbon, and other significant exothermic reactions.

The primary gas in the furnace chamber is carbon monoxide, making up 67.13 wt.% (as indicated in Table S2), with carbon dioxide and nitrogen also present in varying amounts depending on the process stage and air entrainment.

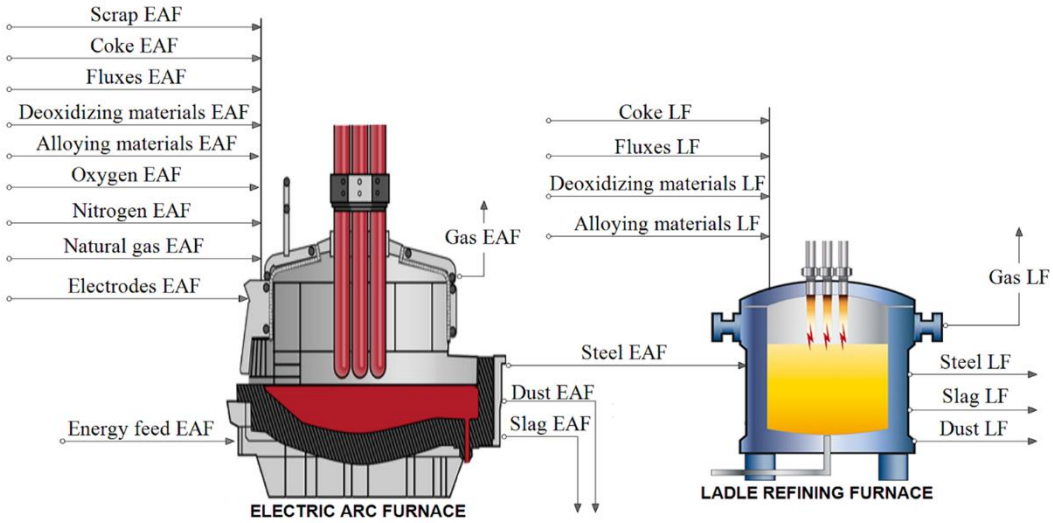

Figure 1. Setting up material flows in an EAF and LF

The input material for EAF consists of a mix of steel scrap of varying quality, bulk density, and surface area-to-volume ratios. The scrap is charged in baskets such that scrap with high bulk density (e.g., foundry return scrap) is placed at the bottom to accelerate heat transfer from the hot bath towards the scrap. Scrap with low bulk density (e.g., sheet metal) is placed at the top of the basket, allowing it to come directly into contact with the electric arc, absorb radiant energy, and melt quickly. After the scrap melts, liquid steel is tapped, leaving about 5-10% of liquid metal from the total furnace capacity for easier melting of new feed, which reduces overall energy consumption. The charging baskets range from 10 to 30 tons, and the charging time per basket is about five minutes. Two to three baskets are charged per cycle. The time from tap to tap is about 50 minutes. The typical strategy for one melting cycle is as follows:

1. Charging the scrap into the furnace, where liquid metal from the previous melt was left,
2. Melting,
3. Second charging,
4. Melting,
5. Third charging,
6. Melting,
7. Refining,
8. Temperature adjustment, and deoxidation (when required, depending on the product grade),
9. Tapping.

The strategy for melting the scrap also affects energy consumption, with losses most associated with interruptions in operation. This can arise due to various factors such as preparation of the tap hole, refractory materials, and problems with charging. Additional materials such as coke and lime are added to the furnace to control composition and foaming of the slag. Foamy slag has multiple contributions to the melting process in the electric arc furnace, such as controlling the oxidation and reduc-

tion of iron, carbon and impurities, preserving refractory material from the radiation of the electric arc, and improving the energy transfer from the electric arc to steel.

2.2. Machine learning methods for obtaining element distribution coefficients

The approach to determining element distribution coefficients in the recycling process of EAF leverages the integration of machine learning with historical operational data. Utilizing data collected over five years, encompassing approximately 14,800 melts focused solely on reinforcing steel production and monitoring 42 different process parameters, provides a robust dataset for analysis.

The primary computational environment is Python 3.x, with libraries such as Pandas for data manipulation and SciPy for mathematical calculations, particularly using the interp1d function for interpolation of slag composition based on lime content.

The methodology begins by conducting five controlled melts in an actual Electric Arc Furnace, with varying amounts of oxygen, coke, and lime in each experiment. These five melts systematically capture the dynamic range of lime additions typically observed in operational settings. Following these adjustments, each melt undergoes detailed chemical analysis in the laboratory to determine the precise chemical compositions of the slag, in line with methods detailed in the literature [10]. This generates foundational data, where results are captured empirically, and derived slag compositions are obtained from each of the five experimental conditions [11].

Utilizing this empirical data, an interpolation method is then applied across all historical entries in the database. This process estimates the slag composition for each melt, leveraging the variations in limestone ($CaCO_3$) addition recorded during actual furnace operations. By interpolating between the established data points from the experimental results, we approximate the chemical composition of slag across the broader dataset, thus enhancing the predictive accuracy of the model concerning slag chemistry variations due to differing limestone inputs. Oxygen and coke additions also affect slag chemistry, but they are not covered in this interpolation model. Despite this, the method has yielded reliable results due to the consistent processing of reinforcing steel and the inclusion of multiple other operational parameters.

This interpolation facilitates the development of predictive models for element transition (distribution), such as alloying components, impurities, and base metals like iron, from liquid steel into slag. By extending the slag content across the entire database based on oxygen, coke, lime addition, a foundation is laid for predictive modeling. For instance, machine learning models, like those predicting the transfer of valuable elements from liquid steel to slag, are developed using Python's sklearn library with RandomForestRegressor. In developing these models, data preparation involves splitting the dataset into training and test sets using the train test split function, with 20% of the data designated as the test set to ensure robust model evaluation. Model parameter optimization is conducted through RandomizedSearchCV, exploring a defined parameter space to identify optimal settings over 50 iterations with three-fold cross-validation. The resulting optimized RandomForestRegressor model is trained on the training set. Model evaluation on the test set utilizes metrics such as Mean Absolute Error (MAE) and the coefficient of determination (R^2) to assess performance, providing insights into the accuracy and reliability of the model's predictions [1, 11-13].

2.3. HSC Chemistry setup

The modeling and simulation of the steel production process was carried out using chemical analysis and determination of the most important thermodynamic parameters of the process. HSC Chemistry version 9 was used to determine material and energy flows. The program contains 24 modules for calculations and one of the modules is HSC-Simulation (HSC-Sim), was used in this work. The model begins with the selection of input raw materials, phase composition, temperature and pressure input from the observed process. The distribution coefficients of the elements in the products are determined on the basis of the equilibrium composition of the observed system and in accordance with the specified reactions in the defined regime. The software provides data for the material and energy balance of the given process, depending on the input conditions, the data of which are stored in the program's database. The modeling results enable a comprehensive analysis of material, which ultimately provides an insight into the overall material and energy input and output flows. An overview of the entire modeling approach has been shown in Figure 2.

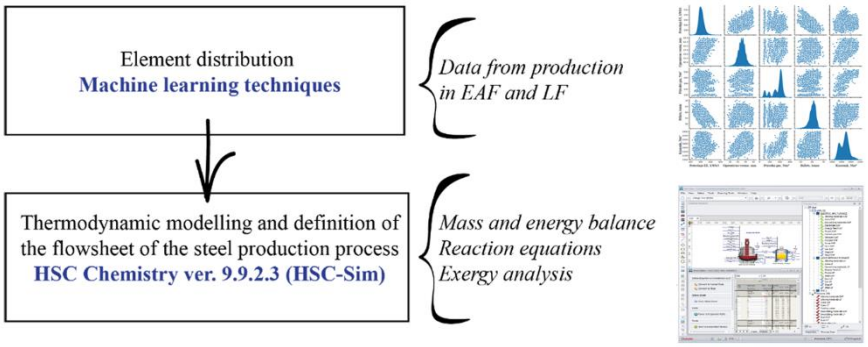

Figure 2. Modeling procedure for performing the exergy analysis

3. Results and discussion

3.1. Elements distribution using machine learning techniques

The integration of predictive machine learning techniques in EAF represents a shift from traditional steel production methods to intelligent, data-driven operations. These models enable real-time adjustments of process parameters based on predictive analytics, significantly enhancing energy efficiency. For instance, the justified use of input materials and fine-tuning of operational parameters, guided by predictive models, not only reduces energy consumption but also maintains the quality of produced steel. Such precision in managing electrical energy consumption directly contributes to reducing environmental footprint in steelmaking, aligning with circular economy principles of waste minimization and environmental impact.

To achieve a comprehensive material balance and accurately determine the distribution coefficients for various elements, machine learning models were trained on extensive historical operational data [1]. This data encompassed a wide range of process parameters, allowing the models to capture the complex relationships between input materials, operational conditions, and output compositions. By leveraging these predictive models, the study could accurately estimate the material flows and element distributions for each melt, resulting in the detailed material balance presented in Table 1.

Table 1. Empirical distribution coefficients obtained using ML techniques on production data

Element	Steel EAF	Slag EAF	Dust EAF	Gas EAF
Al	0.0022	0.9930	0.0048	/
B	1.0000	/	/	/
C	0.0239	/	0.2790	0.6971
Ca	/	0.9538	0.0456	/
Cr	0.6952	0.3048	/	/
Cu	0.9674	0.0016	0.0310	/
Fe	0.9770	0.0205	0.0025	/
H	/	/	/	1.0000
Mg	/	0.6763	0.3237	/
Mn	0.4409	0.5591	/	/
Mo	1.0000	/	/	/
N	/	/	/	1.0000
Ni	1.0000	/	/	/
O	/	0.6210	0.0590	0.3200
P	1.0000	/	/	/
Pb	0.7075	/	0.2925	/
S	0.8892	/	0.1108	/
Si	0.1597	0.8379	0.0024	/
Sn	1.0000	/	/	/
V	1.0000	/	/	/
Zn	0.1097	/	0.8903	/

The distribution of elements between steel, slag, gas, and dust phases in the EAF process reflects the efficiency of the process in managing alloying elements and impurities. The chemical analysis of crude steel is an average based on 8,763 melts related to reinforcing steel production, after applying the cleaning procedure of data described in detail in the reference [1].

3.2. Exergy analysis

Based on the average input data for the variables from production and the distribution coefficients of the elements from Table 1, HSC Chemistry software was used to perform precise thermochemical calculations. The output components were determined according to Table 2 and Figure S1, where the precision of the values reflects the results of the computational model.

Table 2. Streams of the input and output materials in the EAF and LF

Input materials			Output materials		
Component	Mass [kg]	Mole [kmol]	Component	Mass [kg]	Mole [kmol]
Electric arc furnace					
Scrap	64994.0	1218.3	Steel	61174.5	1096.9
Coke	350.0	24.6	Slag	6057.6	76.3
Fluxes	1559.0	16.6	Dust	1148.4	36.5
Deoxidizing materials	4.5	0.17	Gas	2042.3	95.4
Alloying materials	524.5	12.7			

Oxygen Nitrogen Natural gas Electrodes	2701.8 24.6 181.8 84.2	84.4 0.88 11.3 7.01			
Total	70424.5	1376.0		70422.8	1305.2

Ladle refining furnace					
Steel Coke Fluxes Deoxidizing materials Alloying materials	61174.6 214.5 668.3 1.95 224.8	1096.9 15.1 7.10 0.07 5.45	Steel Slag Dust Gas	61349.3 674.8 82.0 178.0	1106.6 11.3 6.57 7.26
Total	62284.1	1124.6		62284.1	1131.6

Based on the results of the simulation and using input material data (Table 2) for EAF and LF, an analysis of the energy of the steel production process was done.

The values of energy are calculated for the mass of components of the input materials, which data is listed in Table 2 and in Tables S1 and S2. The energy calculation for the steel production process detailed is listed in tables S3 and S4, as well as in the following figures 3 and 4.

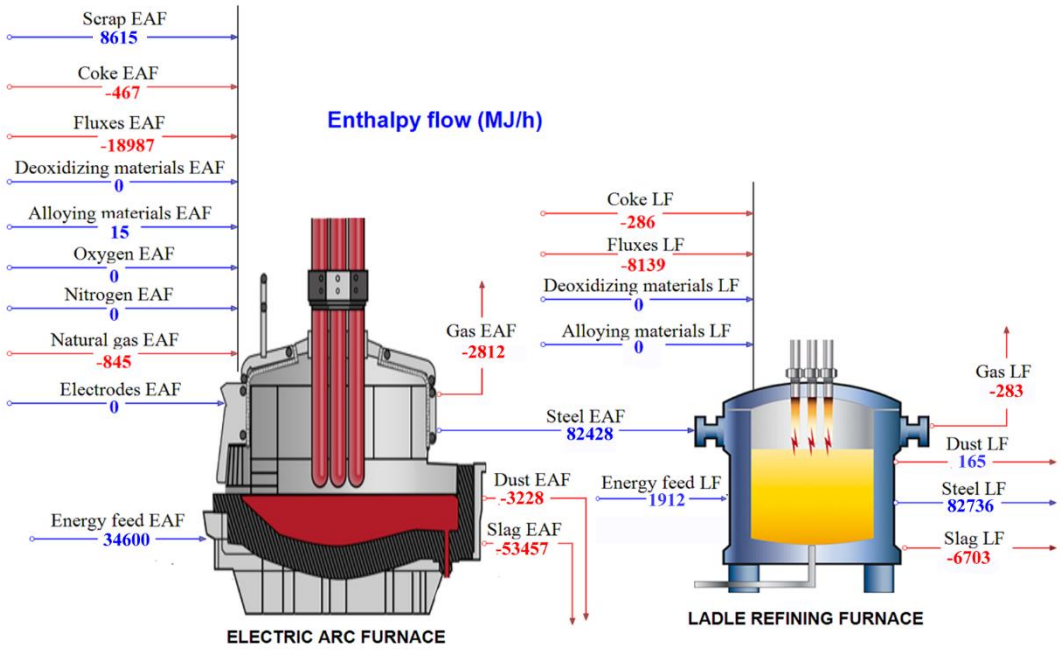

Figure 3. Enthalpy flow for EAF and LF

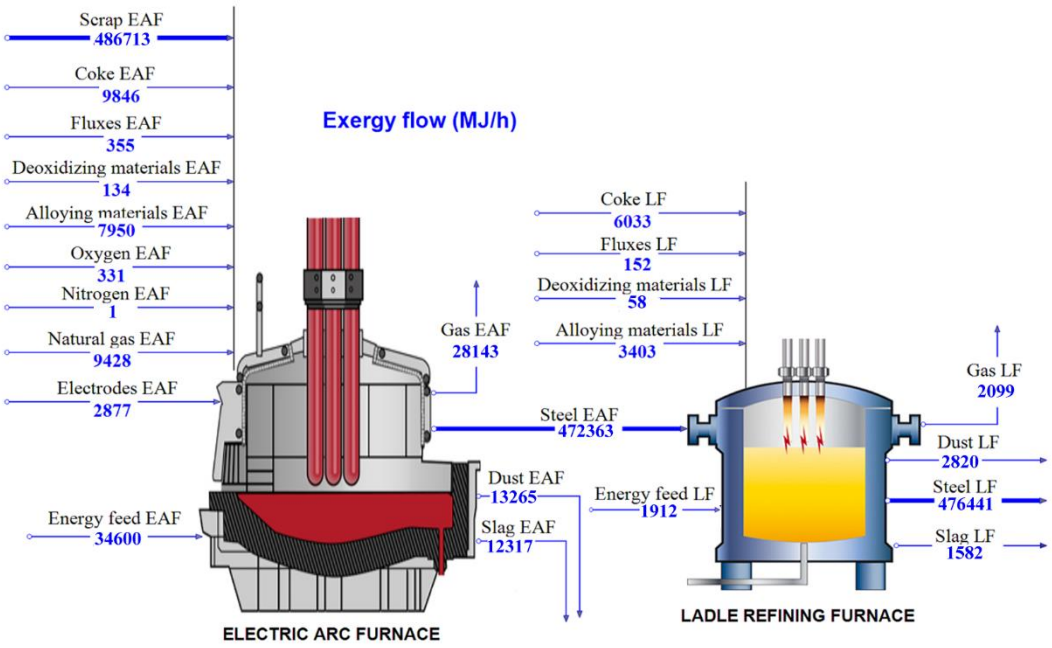

Figure 4. Exergy flow for EAF and LF

Figures 5 to 8 compare the total exergies of the input and output materials, respectively. It should be noted that scrap has the highest total exergy of the input materials and steel has the highest exergy of the output materials.

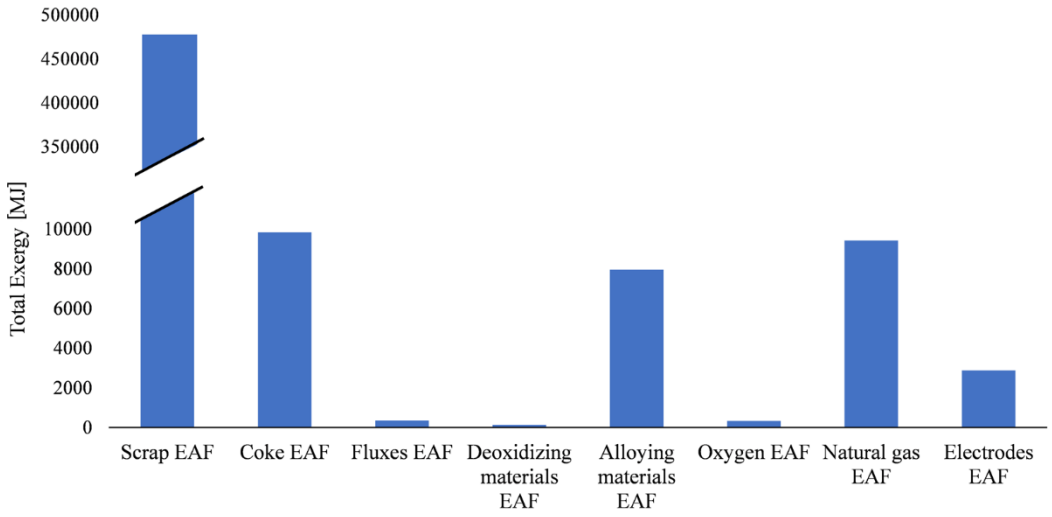

Figure 5. Total exergy of input materials of EAF

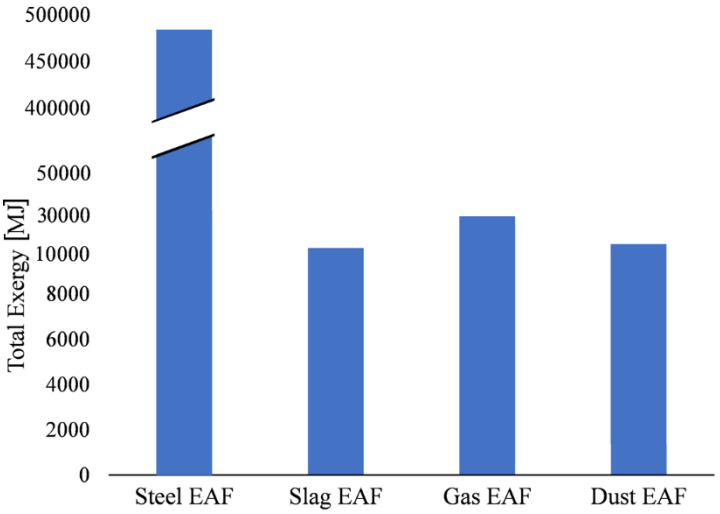

Figure 6. Total exergy of output materials of EAF

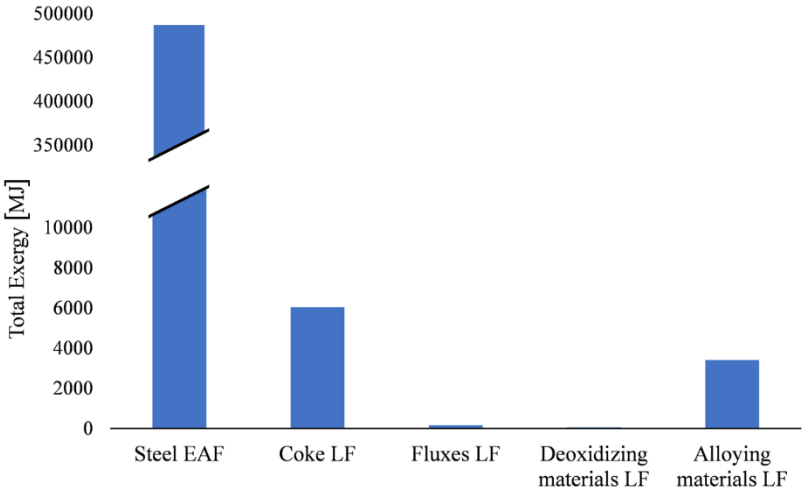

Figure 7. Total exergy of input materials of LF

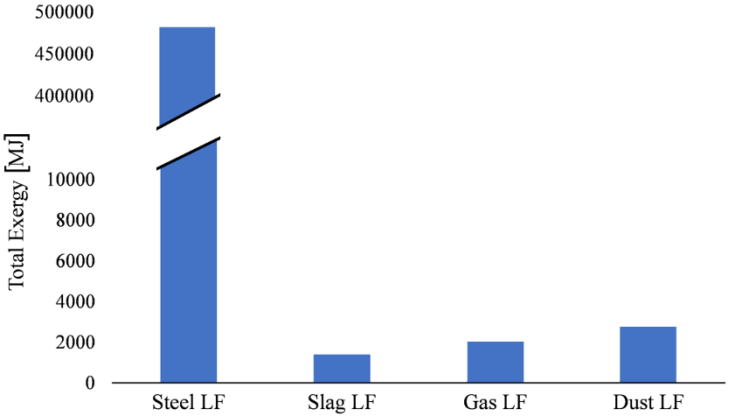

Figure 8. Total exergy of output materials of LF

The calculated results of equilibrium composition for selected elements in the steel phase and slag phase of EAF are shown in the following figures.

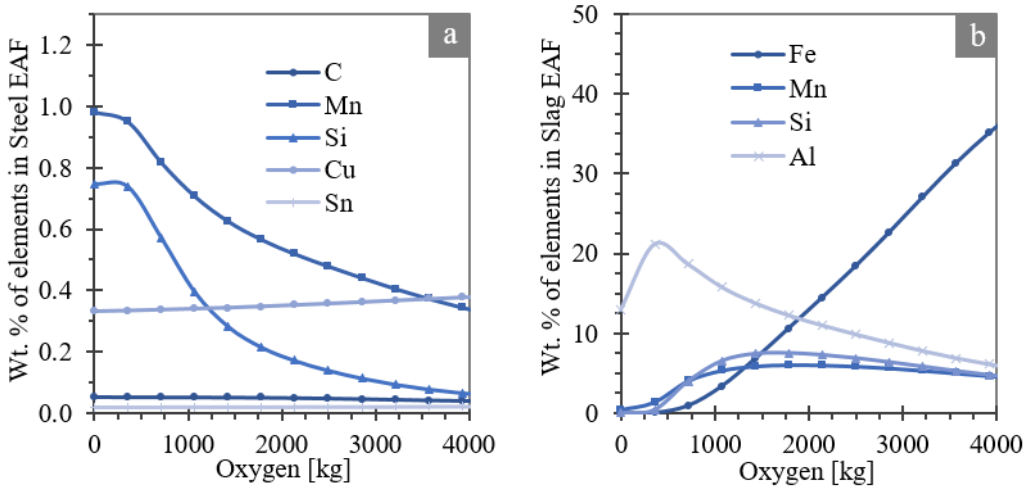

Figure 9. Distribution of elements per Oxygen input in a) Steel EAF and b) Slag EAF at 1600°C

Higher oxygen input during the refining stage leads to the oxidation of alloying elements like silicon and manganese, or aluminum (as impurity from scrap), which have a higher affinity for oxygen than iron. This results in their transfer to the slag. To compensate for these losses, higher quantities of ferrosilicon and ferromanganese are often added during the final stage of the process.

Copper shows higher amount in the steel with increased oxygen use because when the other alloying elements and iron are oxidized preferentially, reducing the mass of alloy, without copper oxidation and therefore it's composition in the molten alloy increases.

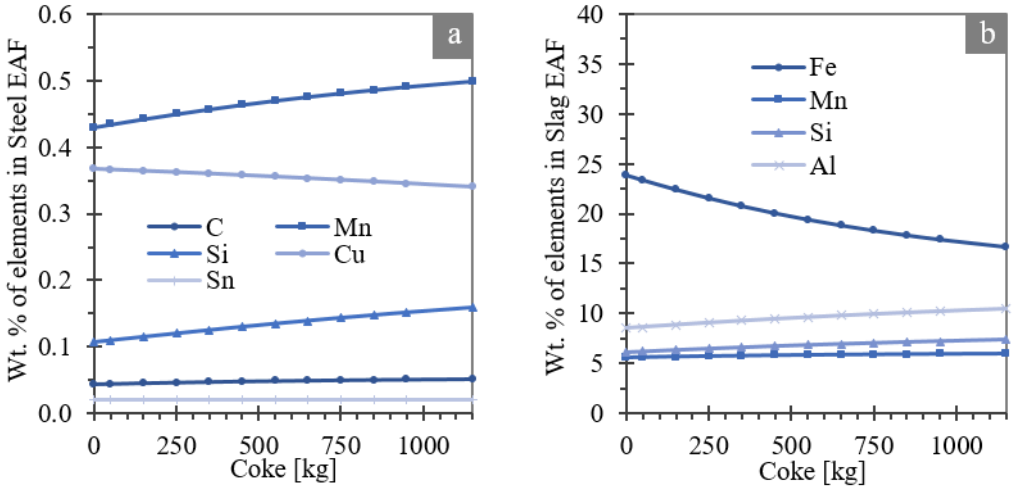

Figure 10. Distribution of elements per Coke input in a) Steel EAF and b) Slag EAF at 1600°C

With an increase in coke input, oxygen is consumed by it, leading to less oxidation of alloying elements to slag and more reporting to molten alloy.

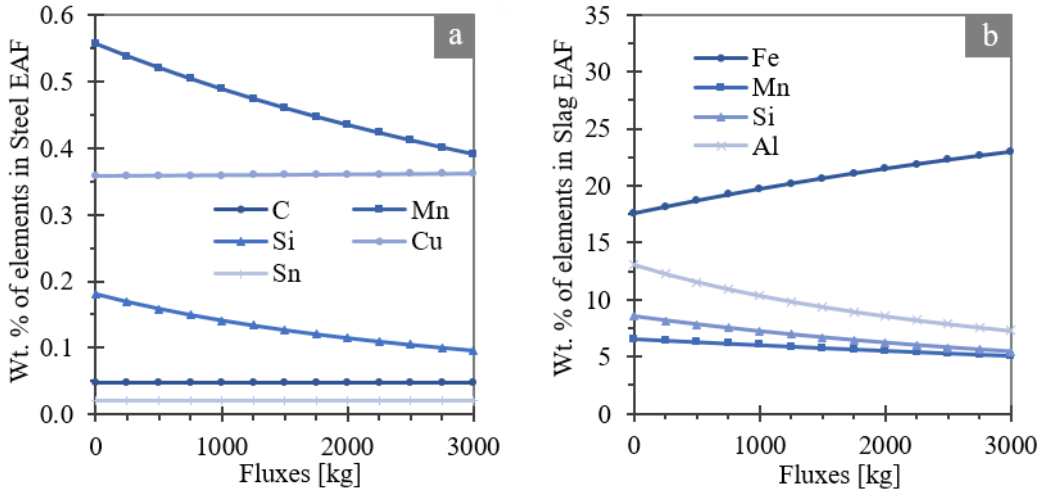

Figure 11. Distribution of elements per Fluxes input in a) Steel EAF and b) Slag EAF at 1600°C

The fluxes used in the EAF process consist of 95.7 wt.% $CaCO_3$ and 4.3 wt.% MgO, with the MgO content coming from recycled refractory material, which is crushed and added back into the furnace. Increased fluxes alter the slag basicity, which enhances its oxidizing capacity, causing more alloying elements like silicon and manganese to report to the slag rather than remaining in the alloy.

The distribution of manganese (Mn) and silicon (Si) in the EAF process is crucial for understanding material losses and optimizing energy use. This significant loss indicates the strong oxidizing conditions within the EAF, which facilitate the formation of silicon dioxide. The presence of Mn and Si in the slag can be influenced by the oxygen potential in the slag phase and the basicity of the slag. By optimizing the input of lime and other fluxes, it is possible to adjust the basicity and reduce manganese losses, thus improving the yield of manganese in the steel phase. Controlling these conditions is important for improving recovery of Mn and Si, and reducing the need for additional alloying materials.

4. CONCLUSION

The integration of exergy analysis with machine learning techniques provides a robust framework for analysis of the EAF steel recycling process. The study highlights the critical balance between material losses and energy consumption, demonstrating that careful control of furnace conditions and input materials can significantly reduce the loss of valuable elements like manganese and silicon. By adjusting the slag composition and the basicity with the oxygen potential, it is possible to improve the recovery of these elements in the steel phase and thus increase the overall yield and quality of the steel produced.

The exergy analysis reveals substantial opportunities for improving energy efficiency, particularly by addressing exergy destruction in the slag and gas phases. This approach not only reduces energy consumption but also minimizes the environmental impact of steel production. The use of machine learning models enables real-time predictions and adjustments, enhancing process control and operational efficiency.

Acknowledgements:

This work was supported by the Ministry of Science, Technological Development and Innovation of the Republic of Serbia (Contract No. 451-03-65/2024-03/200135 and Contract No. 451-03-66/2024-03/200287)

5. REFERENCES

[1] Manojlović, V., et al., Machine learning analysis of electric arc furnace process for the evaluation of energy efficiency parameters, *Applied Energy, 307* (2022), pp. 118209

[2] Graedel, T. E., et al., Alloy information helps prioritize material criticality lists, *Nature Communications, 13* (2022), 1, pp. 150

[3] Reuter A. M., et al., Challenges of the circular economy: a material, metallurgical, and product design perspective, *Annual Review of Materials Research, 49* (2019), 1, pp. 253-274

[4] Antoinette, S., et al., Recycling indices visualizing the performance of the circular economy, *World of Metallurgy-Erzmetall, 69* (2016), 4, pp.201-216

[5] Bhavik, B., et al., *Thermodynamics and the Destruction of Resources*, Cambridge University Press, 2011

[6] Camdali, U., et al., Analysis of an Electric Arc Furnace Used for Casting of Steel: An Exergy Approach, Metallurgist *64* (2020), pp. 483–495

[7] Hajidavalloo, et al., Exergy and energy analysis of an AC steel electric arc furnace under actual conditions, *International Journal of Exergy*, 12 (2013), 3, pp. 380 - 404

[8] Hemal, C., et al., Exergetic sustainability analysis of industrial furnace: a case study, *Environmental Science and Pollution Research, 28* (2021), 10, pp. 12881-12888

[9] Roine, A., and Lamberg, P, HSC Chemistry, vers. 9. Outotec Pori (2020), https://www.hsc-chemistry.com/

[10] Manojlović V., Sokić, M., Ercegović, M., Kamberović, Ž., Ranđelović, D., Zarić, M., Zakonović, J, Technical Solution: Development and application of the XRF method enhanced with machine learning techniques for the determination of slag composition in the steel industry, 2024

[11] Zhang, R., and Jian Y, State of the art in applications of machine learning in steelmaking process modeling, *International Journal of Minerals, Metallurgy and Materials*, *30* (2023), 11, pp. 2055-2075

[12] Zhang, S., et al., Predictive Modeling of the Hot Metal Sulfur Content in a Blast Furnace Based on Machine Learning, *Metals, 13* (2023), 2, pp 288

[13] Forootan, M. M., et al., Machine learning and deep learning in energy systems: A review, *Sustainability, 14* (2022), 8, pp. 4832

Paper submitted: Jun 7, 2024
Paper revised: September 9, 2024
Paper accepted: October 24, 2024

Supplementary materials

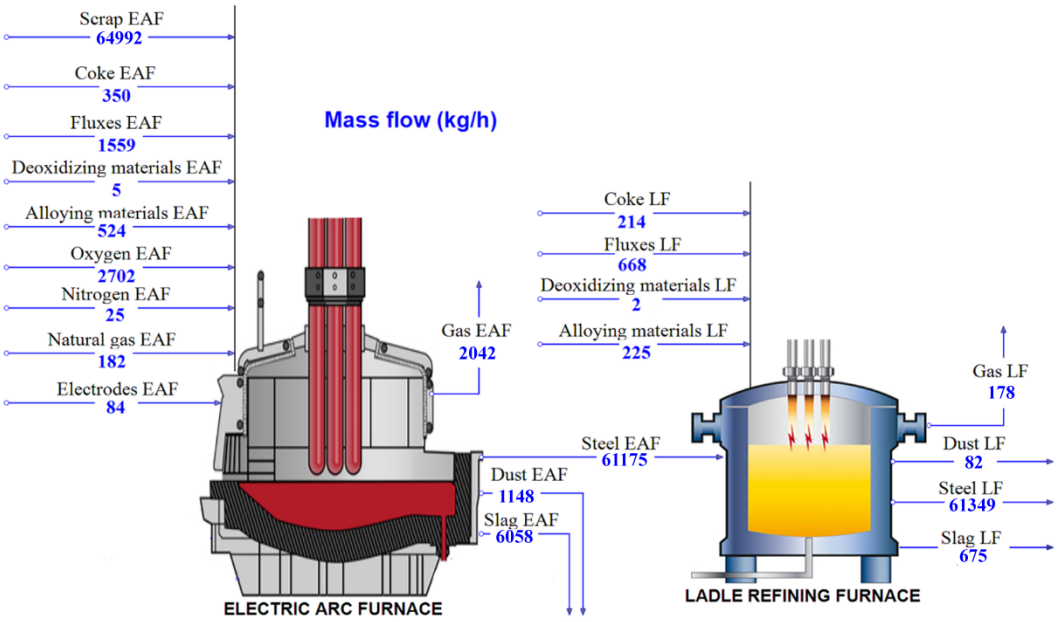

Figure S1. Mass flow for EAF and LF

Table S1. Input materials element composition of EAF

Component	wt. %
	Scrap EAF
Fe(FCC)	94.4000
C	0.7900
Mn	0.5900
Si	0.5000
S	0.0400
P	0.0300
Cr	0.1700
Ni	0.1000
V	0.0040
Zn	0.5500
Pb	0.0500
Cu	0.3500

Sn	0.0200
Mo	0.0200
B	0.0003
Al	0.8600
As	0.0100
Na	0.0100
K	0.0100
Co	0.0100
Cd	0.0020
Ti	0.0600
Nb	0.0040
Sb	0.0100
Zr	0.2900
Bi	0.0100
Ca	0.9200
Mg	0.1800
Ce	0.0020
W	0.0050
Total	100.00
	Coke EAF
C	79.90
S	1.72
SiO_2	2.47
H_2O	2.06
NH_4NO_3	13.84
Total	100.00
	Fluxes EAF
$CaCO_3$	95.72
MgO	4.28
Total	100.00
	Deoxidizing materials EAF
Al	100.00
Total	100.00
	Alloying materials EAF
Fe(FCC)	21.02
Si	28.70
Mn	47.85
C	1.52
P	0.10
S	0.02
Cr	0.07
Al	0.48
Ca	0.24

Total	100.00

Table S2. Output materials element composition of EAF

Component	wt. %
	Steel EAF
Fe	98.1670
C	0.0470
Mn	0.4570
Si	0.1252
P	0.0327
S	0.0467
Ni	0.1062
Cr	0.1260
Cu	0.3597
Mo	0.0212
V	0.0042
Ti	0.0182
Al	0.0021
Nb	0.0042
W	0.0053
As	0.0106
Sn	0.0212
Co	0.0106
Pb	0.0376
B	0.0003
Sb	0.0106
Zr	0.3081
Bi	0.0106
Ca	0.0012
Zn	0.0641
Ce	0.0021
Total	100.00
	Slag EAF
Na_2O	0.14
MgO	2.91
Al_2O_3	17.53
SiO_2	14.19
K_2O	0.13
CaO	26.37
TiO_2	0.77

MnO	7.44
Fe_2O_3	29.70
CuO	0.01
Cr_2O_3	0.82
Total	100.00
	Gas EAF
CO(g)	73.0090
CO_2(g)	0.0003
N_2(g)	1.5555
H_2(g)	0.0000
H_2O(g)	25.4347
Total	100.00
	Dust EAF
Al_2O_3	0.44
C	29.16
CaO	6.66
Cd	0.11
CuS	0.92
MgO	7.35
Mn_3O_4	0.70
PbO	0.89
SiO_2	0.21
$ZnFe_2O_4$	27.28
ZnO	25.08
Fe_3O_4	0.58
Total	100.00

Table S3. Energy values of input streams of EAF on a chemical component basis (T=25°C, p=1atm)

Component	Thermal Energy	Total Enthalpy	Chemical Exergy	Physical Exergy	Total Exergy
	MJ				
Scrap EAF					
Fe(FCC)	8 614.55	8 614.55	411 226.21	5 823.60	417 049.81
C	0.00	0.00	17 538.88	0.00	17 538.88
Mn	0.00	0.00	3 404.12	0.00	3 404.12
Si	0.00	0.00	9 892.98	0.00	9 892.98
S	0.00	0.00	494.01	0.00	494.01
P	0.00	0.00	542.19	0.00	542.19
Cr	0.00	0.00	1 241.83	0.00	1 241.83
Ni	0.00	0.00	268.64	0.00	268.64
V	0.00	0.00	36.81	0.00	36.81

Zn	0.00	0.00	1 884.66	0.00	1 884.66
Pb	0.00	0.00	39.08	0.00	39.08
Cu	0.00	0.00	474.68	0.00	474.68
Sn	0.00	0.00	60.42	0.00	60.42
Mo	0.00	0.00	99.07	0.00	99.07
B	0.00	0.00	11.33	0.00	11.33
Al	0.00	0.00	16 483.69	0.00	16 483.69
As	0.00	0.00	42.73	0.00	42.73
Na	0.00	0.00	95.19	0.00	95.19
K	0.00	0.00	60.96	0.00	60.96
Co	0.00	0.00	34.56	0.00	34.56
Cd	0.00	0.00	3.45	0.00	3.45
Ti	0.00	0.00	739.08	0.00	739.08
Nb	0.00	0.00	25.18	0.00	25.18
Sb	0.00	0.00	23.39	0.00	23.39
Zr	0.00	0.00	2 237.64	0.00	2 237.64
Bi	0.00	0.00	8.55	0.00	8.55
Ca	0.00	0.00	10 877.83	0.00	10 877.83
Mg	0.00	0.00	3 017.51	0.00	3 017.51
Ce	0.00	0.00	9.78	0.00	9.78
W	0.00	0.00	14.65	0.00	14.65
Total	8 614.55	8 614.55	480 889.10	5 823.60	486 712.70
Coke EAF					
C	0.00	0.00	9 552.34	0.00	9 552.34
S	0.00	0.00	114.67	0.00	114.67
SiO_2	0.00	- 131.30	0.36	0.00	0.36
H_2O	0.00	- 114.51	0.38	0.00	0.38
NH_4NO_3	0.00	- 221.25	178.54	0.00	178.54
Total	0.00	- 467.06	9 846.29	0.00	9 846.29
Fluxes EAF					
$CaCO_3$	0.00	-17 990.15	255.93	0.00	255.93
MgO	0.00	- 996.84	98.60	0.00	98.60
Total	0.00	-18 986.99	354.54	0.00	354.54
Deoxidizing materials EAF					
Al	0.00	0.00	134.18	0.00	134.18
Total	0.00	0.00	134.18	0.00	134.18
Alloying materials EAF					
Fe(FCC)	15.48	15.48	738.88	10.46	749.35
Si	0.00	0.00	4 582.48	0.00	4 582.48
Mn	0.00	0.00	2 228.00	0.00	2 228.00
C	0.00	0.00	272.64	0.00	272.64
P	0.00	0.00	14.52	0.00	14.52
S	0.00	0.00	1.54	0.00	1.54
Cr	0.00	0.00	4.25	0.00	4.25
Al	0.00	0.00	74.35	0.00	74.35

Ca	0.00	0.00	22.93	0.00	22.93
Total	15.48	15.48	7 939.60	10.46	7 950.06
Oxygen EAF					
O_2(g)	0.00	0.00	330.98	0.00	330.98
Total	0.00	0.00	330.98	0.00	330.98
Nitrogen EAF					
N_2(g)	0.00	0.00	0.59	0.00	0.59
Total	0.00	0.00	0.59	0.00	0.59
Natural gas EAF					
CH_4(g)	0.00	- 845.38	9 428.18	0.00	9 428.18
Total	0.00	- 845.38	9 428.18	0.00	9 428.18
Electrodes EAF					
C	0.00	0.00	2 877.19	0.00	2 877.19
Total	0.00	0.00	2 877.19	0.00	2 877.19
OVERALL	8 630.03	22 930.53	511 800.64	5 834.06	552 234.64

Table S4. Energy values of output streams of EAF on a chemical component basis (T=1600 °C, p= 1 atm)

Compo-nent	Thermal Energy	Total Enthalpy	Chemical Exergy	Physical Exergy	Total Exergy
	MJ				
Steel EAF					
Fe	81 059.68	81 059.68	402 505.67	57 311.62	459 817.28
C	77.40	77.40	981.35	53.58	1 034.93
Mn	403.16	403.16	2 481.86	284.73	2 766.59
Si	249.59	249.59	2 330.80	187.85	2 518.66
P	27.20	27.20	556.72	17.50	574.22
S	47.28	47.28	542.59	30.08	572.67
Ni	79.04	79.04	268.64	55.93	324.57
Cr	80.72	80.72	866.29	55.48	921.77
Cu	204.64	204.64	459.22	141.65	600.87
Mo	6.21	6.21	99.07	4.15	103.22
V	2.52	2.52	36.81	1.70	38.51
Ti	12.58	12.58	210.79	8.50	219.29
Al	2.73	2.73	37.05	1.83	38.87
Nb	1.26	1.26	25.18	0.84	26.01
W	0.78	0.78	14.65	0.52	15.16
As	5.96	5.96	42.73	4.08	46.81
Sn	5.69	5.69	60.42	3.51	63.94
Co	8.27	8.27	34.56	5.90	40.47
Pb	5.59	5.59	27.65	3.57	31.22
B	0.69	0.69	11.33	0.47	11.80
Sb	3.71	3.71	23.39	2.48	25.87
Zr	106.62	106.62	2 237.64	70.99	2 308.64

Bi	1.80	1.80	8.55	1.12	9.66
Ca	1.12	1.12	12.93	0.75	13.69
Zn	33.13	33.13	206.77	21.56	228.33
Ce	0.59	0.59	9.78	0.40	10.19
Total	82 427.95	82 427.95	414 092.44	58 270.81	472 363.25
			Slag EAF		
Na_2O	29.68	- 29.00	42.27	20.87	63.15
MgO	346.81	-2 285.92	260.42	231.38	491.80
Al_2O_3	2 014.16	-15 439.67	156.30	1 355.88	1 512.18
SiO_2	1 581.65	-11 450.29	35.44	1 062.31	1 097.75
K_2O	0.00	0.00	0.00	0.00	0.00
CaO	0.00	0.00	0.00	0.00	0.00
TiO_2	15.30	- 14.89	34.35	10.22	44.57
MnO	2 299.77	-15 782.86	3 638.70	1 519.69	5 158.39
Fe_2O_3	67.45	- 482.70	12.64	44.90	57.54
CuO	544.03	-1 903.40	805.76	362.46	1 168.23
Total	10 492.26	-53 456.72	5 155.67	7 161.06	12 316.73
			Gas EAF		
CO(g)	3 633.45	-4 069.05	19 165.45	2 413.76	21 579.21
CO_2(g)	0.03	- 0.10	0.01	0.02	0.02
N_2(g)	76.58	76.58	0.99	50.86	51.86
H_2(g)	0.00	0.00	0.00	0.00	0.00
H_2O(g)	1 180.44	1 180.44	5 731.80	779.72	6 511.52
Total	7605.39	-10831.38	24 898.25	3 244.38	28 142.63
			Dust EAF		
Al_2O_3	9.64	- 73.88	0.75	6.49	7.24
C	902.10	902.10	11 438.35	624.51	12 062.86
CaO	110.05	- 755.25	174.12	72.72	246.84
Cd	0.61	0.61	3.45	0.39	3.84
CuS	11.39	5.49	76.38	7.72	84.10
MgO	165.96	-1 093.87	124.62	110.72	235.34
Mn_3O_4	15.67	- 33.34	6.62	11.33	17.96
PbO	5.42	- 4.58	2.87	3.72	6.59
SiO_2	4.54	- 32.88	0.10	3.05	3.15
$ZnFe_2O_4$	0.00	0.00	0.00	0.00	0.00
ZnO	395.31	-1 182.44	25.39	263.21	288.60
Fe_3O_4	291.30	- 941.50	100.92	194.55	295.47
Total	1 925.34	-3 228.50	11 957.00	1 307.94	13 264.94
OVERALL	99 736.11	22 930.53	456 103.36	69 984.19	526 087.55